

Electronic Supplementary Information

Well-designed hierarchical $\text{Bi}_{19}\text{S}_{27}\text{Br}_3$ nanorods@ SnIn_4S_8 nanosheets core-shell S-scheme heterostructure for robust photothermal-assisted photocatalytic CO_2 reduction

Weifeng Jia, Renzhi Xiong, Yiting Sun, Yanhe Xiao, Baochang Cheng and Shuijin Lei*

School of Physics and Materials Science, Nanchang University, Nanchang 330031, China

*To whom correspondence should be addressed. E-mail: shjlei@ncu.edu.cn



Fig. S1 The CEL-SPH2N-D9 automatic photocatalytic activity evaluation system.

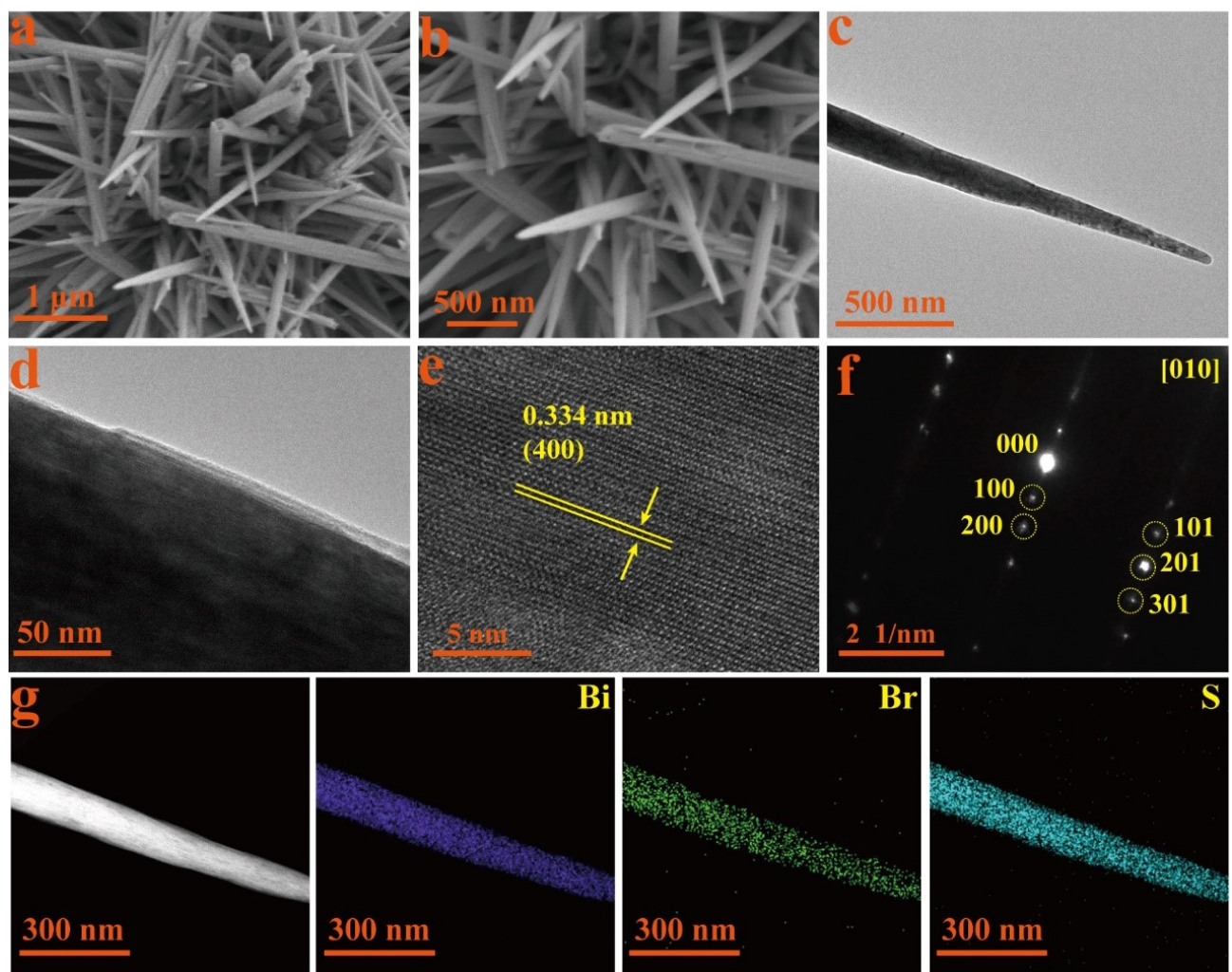


Fig. S2 (a-b) SEM images, (c-d) TEM images, (e) HRTEM image, (f) SAED patterns, and (g) the corresponding EDS elemental mapping images of the prepared $\text{Bi}_{19}\text{S}_{27}\text{Br}_3$ sample.

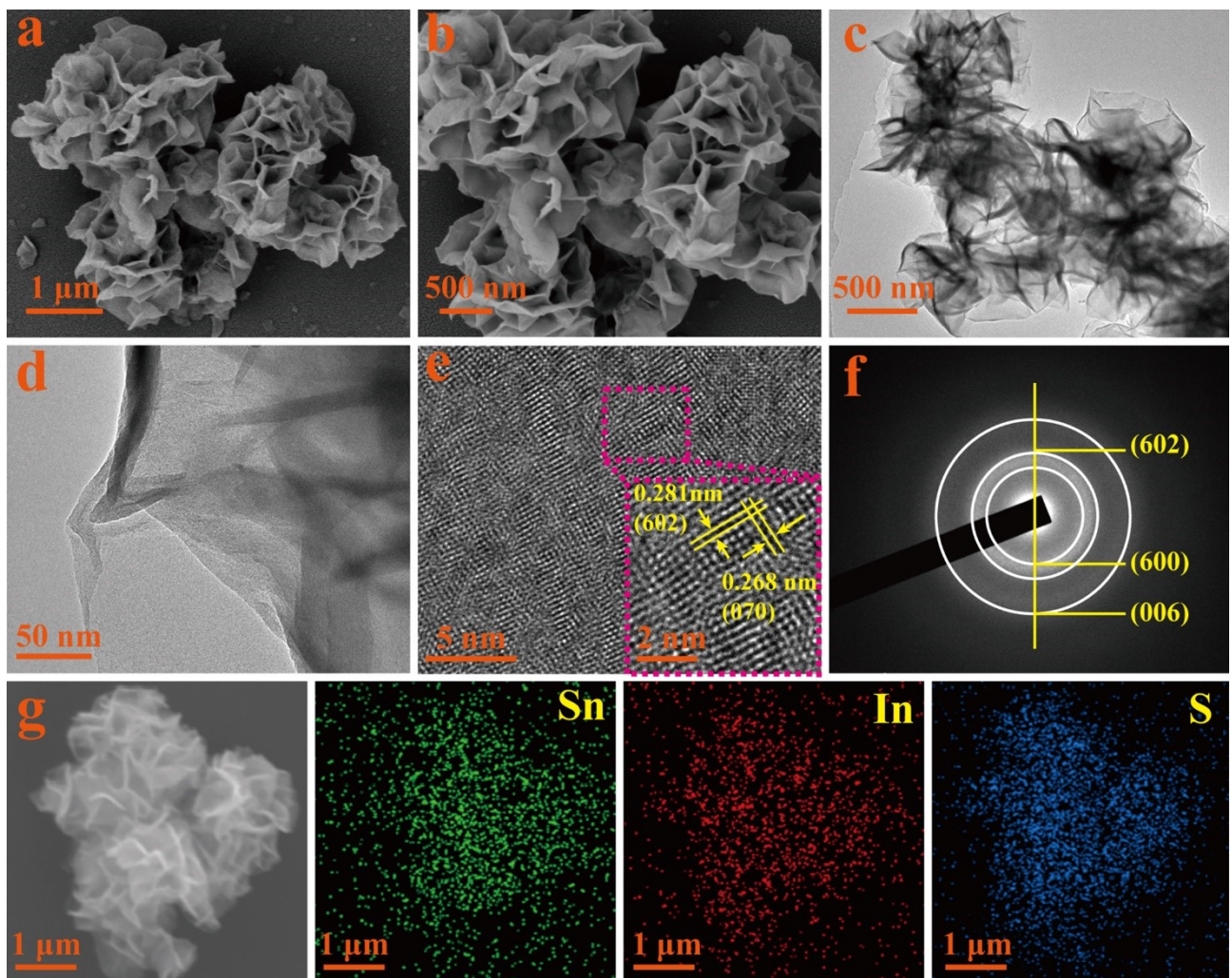


Fig. S3 (a-b) SEM images, (c-d) TEM images, (e) HRTEM image, (f) SAED patterns, and (g) the corresponding EDS elemental mapping images of the prepared SnIn_4S_8 sample.

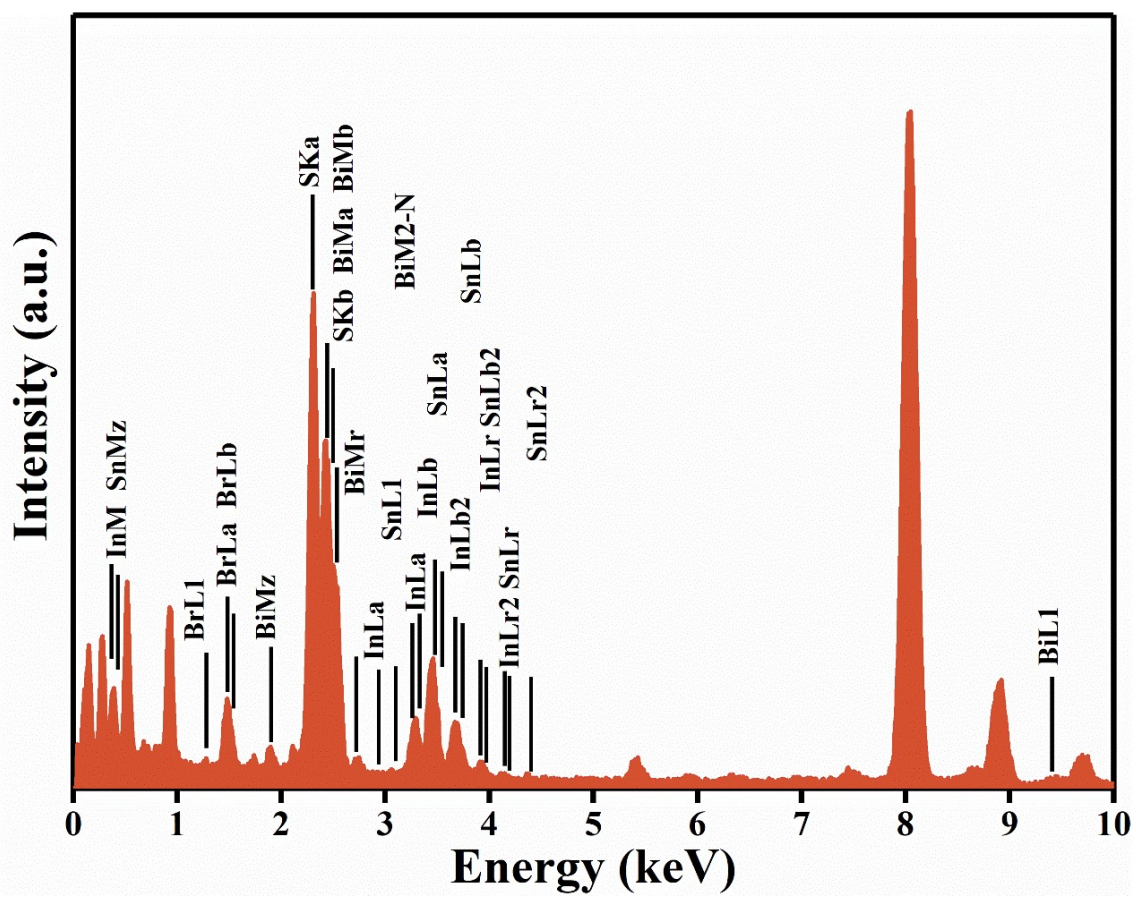


Fig. S4 EDS spectrum of the prepared BSB@SIS-3 composite sample.

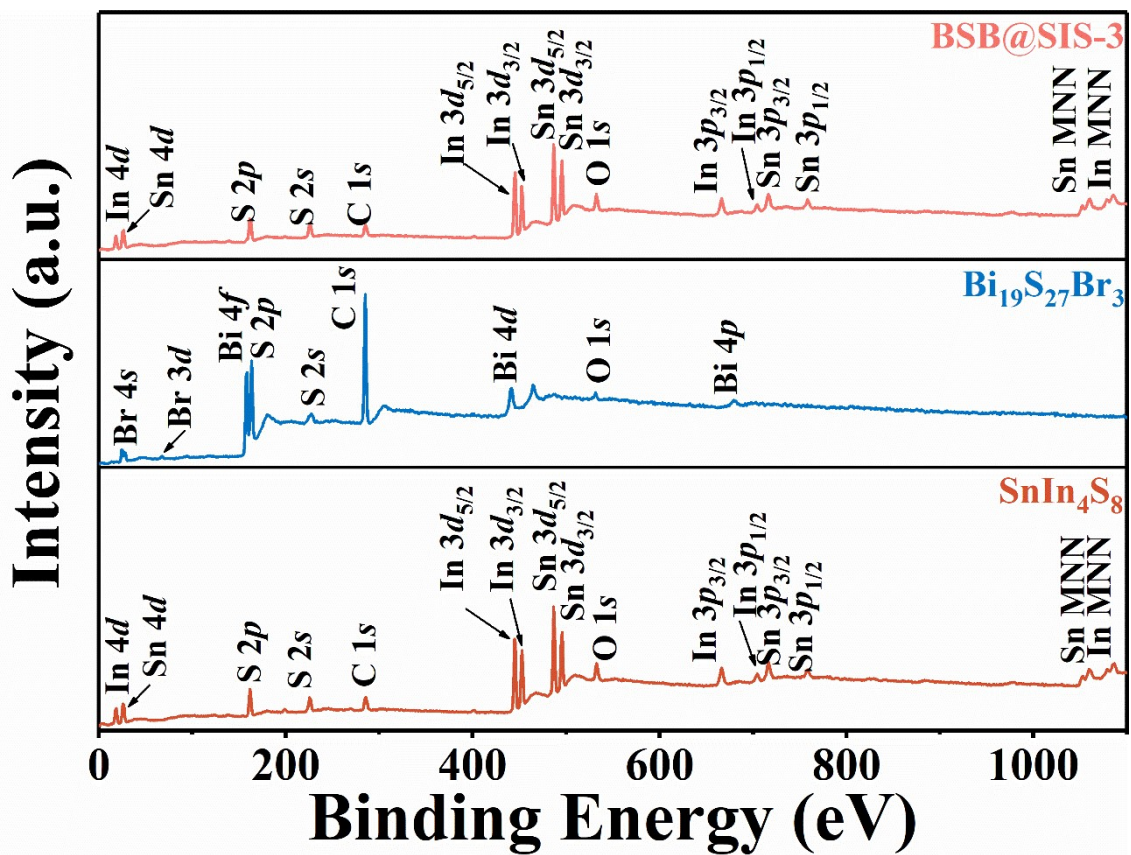


Fig. S5 XPS survey spectra of the prepared SnIn_4S_8 , $\text{Bi}_{19}\text{S}_{27}\text{Br}_3$ and BSB@SIS-3 samples.

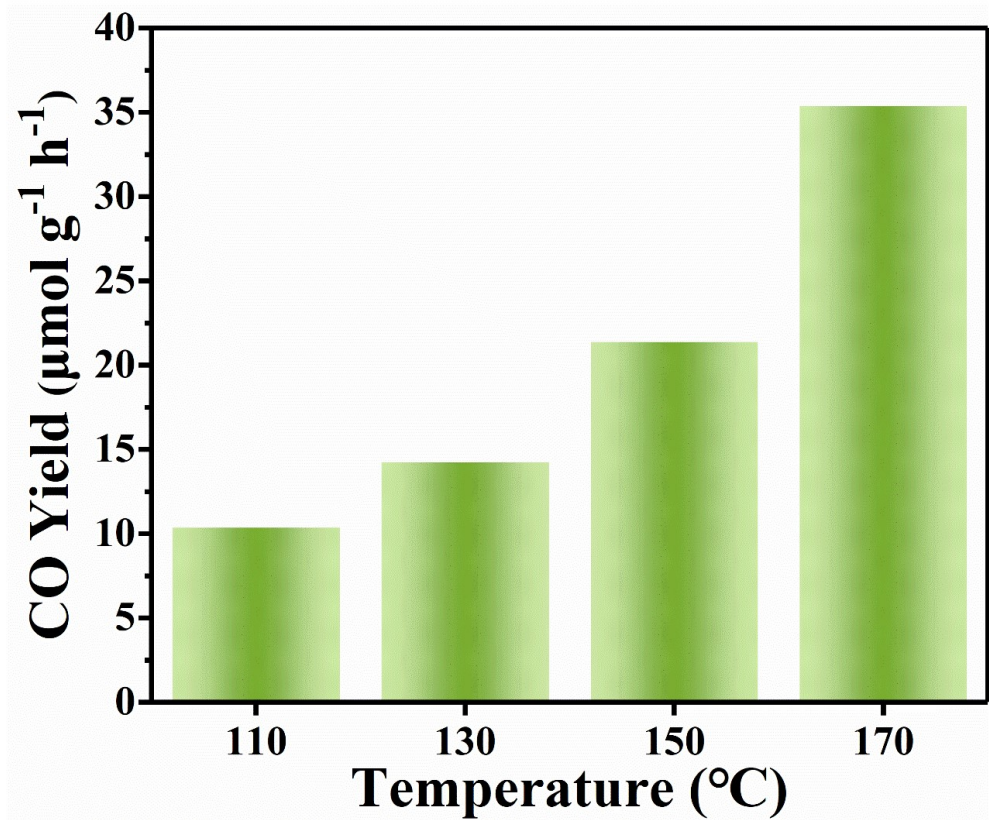


Fig. S6 CO yield of photocatalytic CO_2 reduction under different applied temperatures over the prepared BSB@SIS-3 catalyst.

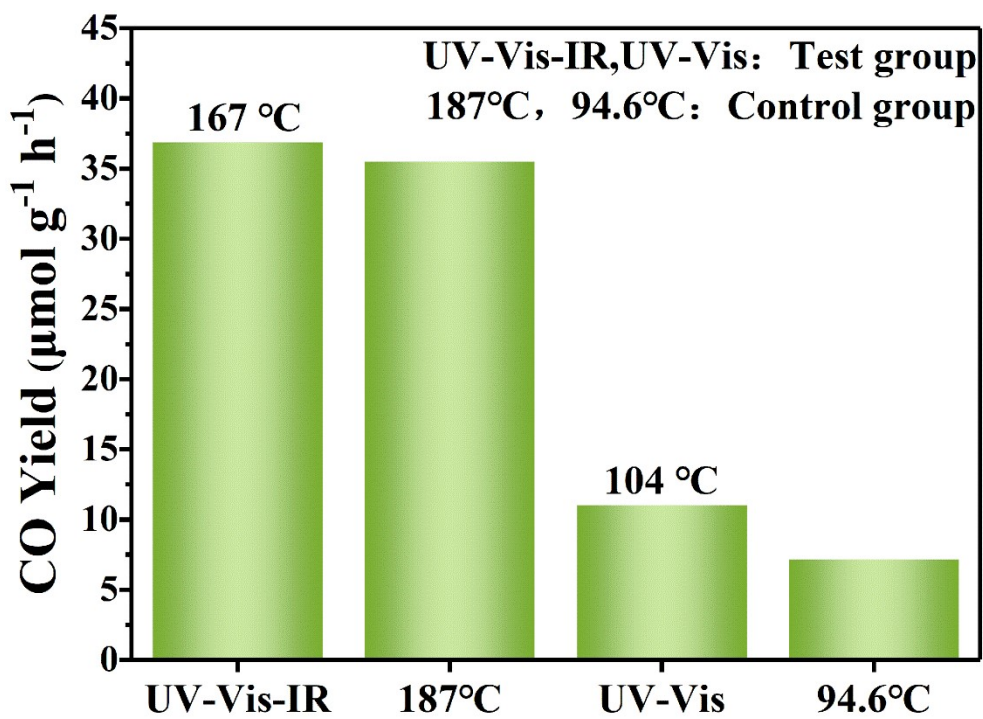


Fig. S7 CO yield of photocatalytic CO_2 reduction at 94.6 °C and 187 °C over the prepared BSB@SIS-3 catalyst.

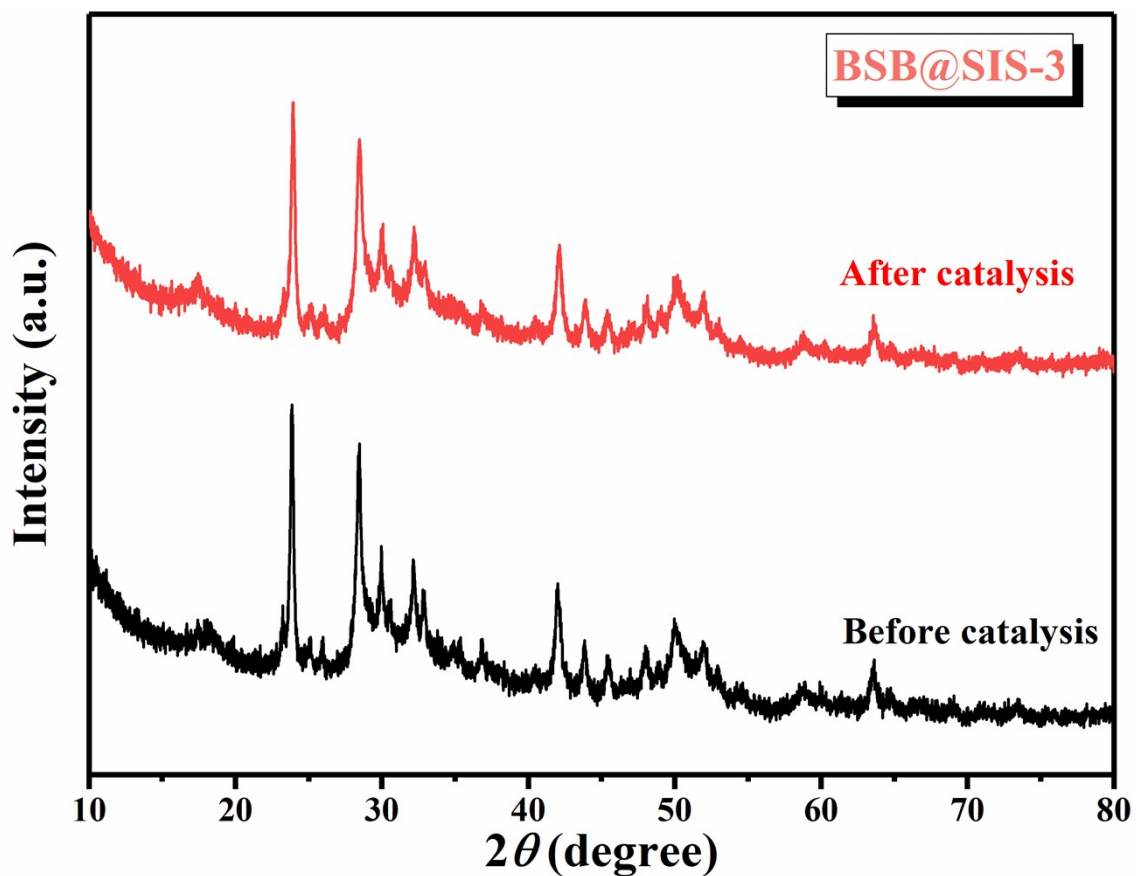


Fig. S8 XRD patterns of the prepared BSB@SIS-3 catalyst before and after five runs of photothermal-assisted photocatalytic CO_2 reduction under UV-Vis-NIR illumination.

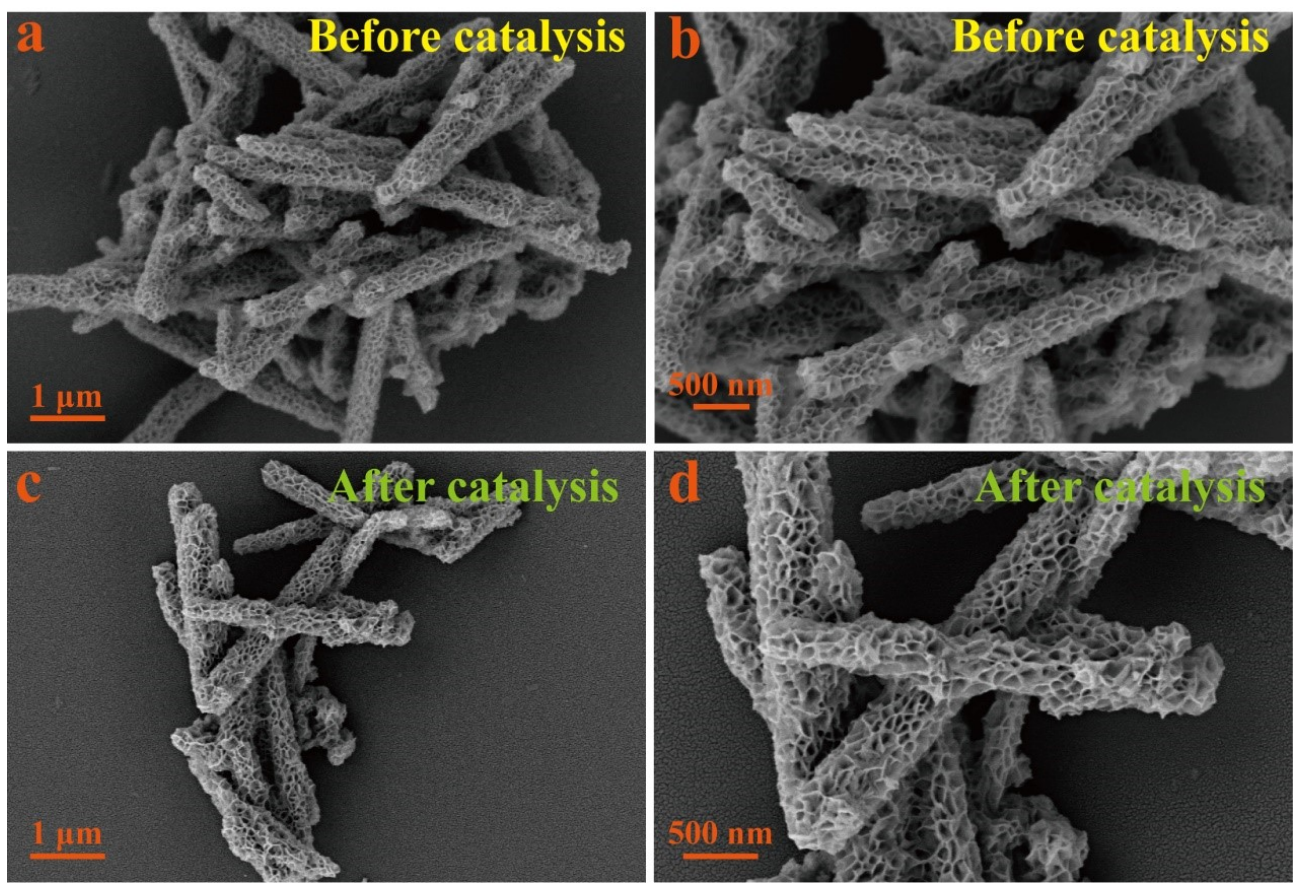


Fig. S9 SEM images of the prepared BSB@SIS-3 catalyst (a-b) before and (c-d) after five runs of photothermal-assisted photocatalytic CO₂ reduction under UV-Vis-NIR illumination.

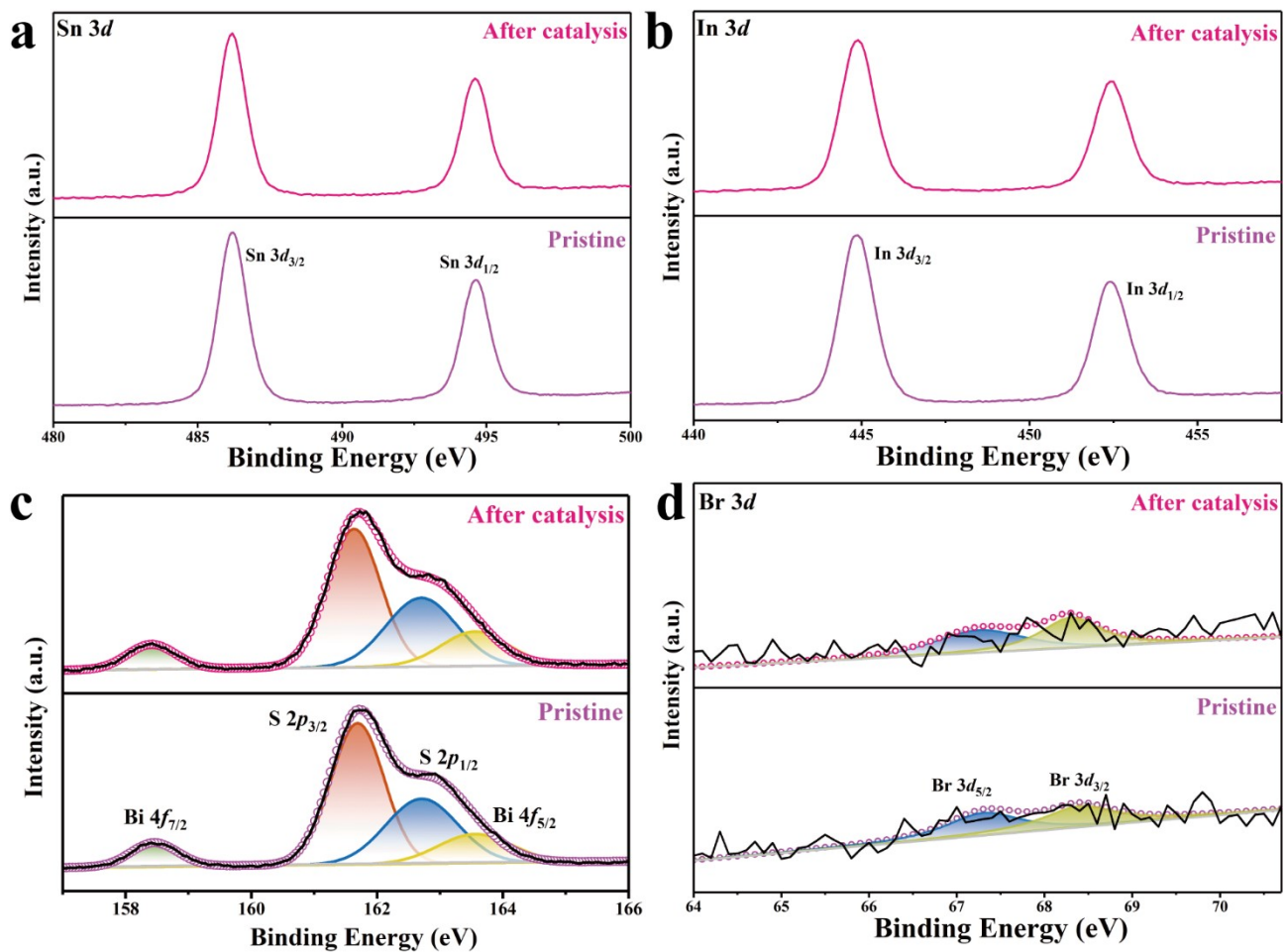


Fig. S10 XPS core-level spectra of (a) Sn 3d, (b) In 3d, (c) Bi 4f & S 2p and (d) Br 3d for the prepared BSB@SIS-3 catalyst before and after five runs of photothermal-assisted photocatalytic CO₂ reduction under UV-Vis-NIR illumination.

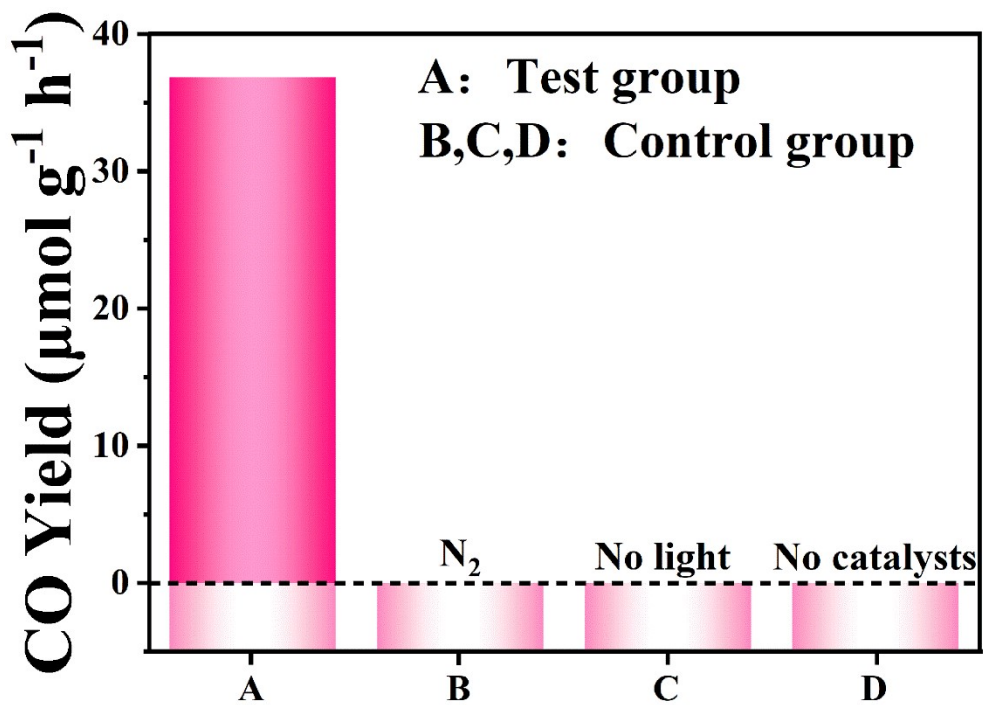


Fig. S11 Control experiments of photocatalytic CO_2 reduction over BSB@SIS-3 under the given conditions of pure nitrogen atmosphere, no light, and no photocatalyst.

Table S1 The element contents of BSB@SIS-3 composite.

Element	wt%	at%	Molar ratio
Bi	43.97	19.13	
Br	2.62	2.98	
S	17.78	50.42	$\text{Bi}_{19}\text{S}_{27}\text{Br}_3:\text{SnIn}_4\text{S}_8 \approx 1:22$
Sn	28.70	21.98	
In	6.93	5.49	

Table S2 Comparison of the photocatalytic CO₂ reduction performance between the prepared Bi₁₉S₂₇Br₃@SnIn₄S₈ S-scheme heterostructure and other reported composite photocatalysts.

Catalyst	Light source	System	Yield of product ($\mu\text{mol g}^{-1} \text{h}^{-1}$)	Ref.
Bi ₁₉ S ₂₇ Br ₃ @SnIn ₄ S ₈	300 W Xe lamp UV-Vis-NIR	CO ₂ + Fiberglass, 5 °C, 70 Kpa	CO: 36.8	This work
Bi ₁₉ S ₂₇ Br ₃ /g-C ₃ N ₄	300 W Xe lamp $\lambda \geq 420$ nm	CO ₂ + H ₂ O, 5 °C, 80 Kpa	CO: 12.87	S1
CdS/Bi ₂ WO ₆ -S	300 W Xe lamp 800 nm $\geq \lambda \geq 420$ nm	CO ₂ + ethyl acetate + isopropyl alcohol	CO: 6.87 CH ₄ : 0.6	S2
V-Bi ₁₉ Br ₃ S ₂₇	300 W Xe lamp	CO ₂ + Glass, 105 Kpa	$\lambda \geq 420$ nm, CH ₄ : 0.65 $\lambda \geq 720$ nm, CH ₃ OH: 0.4	S3
Bi ₁₉ S ₂₇ Br ₃ /BiOBr	300 W Xe lamp $\lambda \geq 420$ nm	CO ₂ + H ₂ O, 80 Kpa	CO: 19.83	S4
PNS-ZnO@g-C ₃ N ₄	300 W Xe lamp $\lambda \geq 420$ nm	CO ₂ + H ₂ O + ITO, 200 °C	CO: 16.8 CH ₄ : 30.5	S5
ZSM-5@NiV ₂ Se ₄	300 W Xe lamp UV-Vis-NIR	CO ₂ + H ₂ O + Glass, 25 °C	C ₂ H ₆ : 4.25	S6
α -Fe ₂ O ₃ /g-C ₃ N ₄	300 W Xe lamp $\lambda \geq 420$ nm	NaHCO ₃ + H ₂ SO ₄ + H ₂ O, 20 °C	CO: 27.2	S7
CdS: Dy/g-C ₃ N ₄	300 W Xe lamp $\lambda \geq 420$ nm	CO ₂ + H ₂ O	CO: 23.44 CH ₄ : 8.06	S8
Bi ₁₉ S ₂₇ Br ₃ /CoAl-LDH	300 W Xe lamp $\lambda \geq 420$ nm	CO ₂ + H ₂ O + triethanolamine	CO: 17.28 CH ₄ : 0.79	S9

References

- S1 J. Zhao, M. Ji, H. Chen, Y. Weng, J. Zhong, Y. Li, S. Wang, Z. Chen, J. Xia and H. Li, *Appl. Catal. B: Environ.*, 2022, **307**, 121162.
- S2 M. Hao, D. Wei and Z. Li, *Energ. Fuel.*, 2022, **36**, 11524–11531.
- S3 J. Li, W. Pan, Q. Liu, Z. Chen, Z. Chen, X. Feng and H. Chen, *J. Am. Chem. Soc.*, 2021, **143**, 6551–6559.
- S4 J. Zhao, M. Xue, M. Ji, B. Wang, Y. Wang, Y. Li, Z. Chen, H. Li and J. Xia, *Chin. J. Catal.*, 2022, **43**, 1324–1330.
- S5 Q. Guo, L. Fu, T. Yan, W. Tian, D. Ma, J. Li, Y. Jiang and X. Wang, *Appl. Surf. Sci.*, 2020, **509**, 144773.
- S6 Y. Tian, R. Wang, S. Deng, Y. Tao, W. Dai, Q. Zheng, C. Huang, C. Xie, Q. Zeng, J. Lin and H. Chen, *Nano Lett.*, 2023, **23**, 10914–10921.
- S7 Z. Jiang, W. Wan, H. Li, S. Yuan, H. Zhao and P. K. Wong, *Adv. Mater.*, 2018, **30**, 1706108.
- S8 Y. Zhao, Z. Han, G. Gao, W. Zhang, Y. Qu, H. Zhu, P. Zhu and G. Wang, *Adv. Funct. Mater.*, 2021, **31**, 2104976.
- S9 J. Hua, C. Ma, D. Wu, H. Huang, X. Dai, K. Wu, H. Wang, Z. Bian and S. Feng, *J. Alloy. Compd.*, 2024, **970**, 172516.